INFLUENCE OF CELLULOSE POLYMERIZATION DEGREE AND CRYSTALLINITY ON KINETICS OF CELLULOSE DEGRADATION

Edita Jasiukaitytė-Grojzdek,*[a,b] Matjaž Kunaver,[a,b] Ida Poljanšek,[a,c]

Cellulose was treated in ethylene glycol with *p*-toluene sulfonic acid monohydrate as a catalyst at different temperatures. At the highest treatment temperature (150 °C) liquefaction of wood pulp cellulose was achieved and was dependant on cellulose polymerization degree (DP). Furthermore, the rate of amorphous cellulose weight loss was found to increase with cellulose degree of polymerization, while the rate of crystalline cellulose weight loss was reciprocal to the size of the crystallites. The cellulose degradation was studied by monitoring of the molecular mass decrease by size-exclusion chromatography. It was revealed that microcrystalline cellulose degrades via a 'quantum mode' mechanism, while the degradation of Whatman filter paper no 1. and cotton linters proceeded randomly and were partly dependent on the starting polymerization degree, crystallinity, and treatment temperature. The kinetics of cellulose degradation in heterogeneous media was described by means of a one-stage model, characterised by the consumption of glycosidic bonds in amorphous and crystalline cellulose regions until the levelling-off degree of polymerization is reached.

Keywords: Cellulose; Acid-catalyzed degradation; 'Quantum mode' mechanism; Ethylene glycol; p-Toluene sulfonic acid monohydrate; Kinetics

*Contact information: a: Center of Excellence for Polymer Materials and Technologies, Tehnološki Park 24, SI-1000 Ljubljana, Slovenia; b: National Institute of Chemistry, Hajdrihova 19, SI-1000, Ljubljana, Slovenia; c: University of Ljubljana, Biotechnical Faculty, Rožna dolina C VIII/34, SI-1000 Ljubljana, Slovenia; * Corresponding author: edita.jasiukaityte@ki.si*

INTRODUCTION

Thermochemical conversion of lignocellulose into a potential feedstock for the synthesis of new, environmentally friendly polymers can be achieved in a liquefaction process under the acidic conditions with phenol or polyhydric alcohols (Lin *et al.* 1994; Alma *et al.* 1998; Lin *et al.* 1995; Kunaver *et al.* 2010). The efficiency of lignocellulosic biomass liquefaction is mostly governed by the recalcitrance of the semicrystalline cellulose to biological and chemical degradation. The high crystallinity and/or high degree of polymerization (DP) tend to constrain cellulose degradation during the liquefaction reaction by inhibiting the penetration of the liquefying agent, especially into the tightly packed crystalline cellulose regions. Several authors (Yamada and Ono 1999; Pan *et al.* 2007; Zhang *et al.* 2007) have confirmed that, independent of the reaction conditions and lignocellulosic material, not-degraded/liquefied residue was composed mainly of cellulose.

Besides the inherent recalcitrance of cellulose, the efficiency of lignocellulose liquefaction also is governed by polycondensation reactions between the depolymerized

cellulose and aromatic lignin derivatives, which otherwise induce the formation of the new residue observed in sulfuric acid-catalyzed liquefaction (Kobayashi *et al.* 2004). Formation of high-molecular mass structures designated as 'lignin-based polymer' during *p*-toluene sulfonic acid-catalyzed (PTSA-catalyzed) wood liquefaction was an objective of the extensive study performed by Jasiukaitytė *et al.* (2010). The cited authors reported on improved solubility of high-molecular mass structures of 'lignin-based polymer' in the reaction medium. The principal advantage of the PTSA-catalyzed liquefaction is a restriction of the intensive polycondensation reactions. The restriction is achieved by lowering the hydronium ion concentration from 0.009 mol/L in H_2SO_4 to 0.0023 mol/L in PTSA. Additionally, it was demonstrated that, independent of the type of catalyst used, a similar extent of the cellulose liquefaction was achieved (Jasiukaitytė *et al.* 2009).

Cellulose degradation is considered to be a rate-determining step of lignocellulose liquefaction. There is a great influence of physical structural features of cellulose that differ among various lignocellulosic materials such as softwood, hardwood, corn stover, rice and wheat straw, and bagasse. Crystallinity and cellulose degree of polymerization are important factors for the yield of cellulose liquefaction in acidified ethylene glycol. However, particularly rapid amorphous cellulose depolymerization followed by partial degradation of crystalline domains proceeded without dependence on the starting molecular mass (Jasiukaitytė *et al.* 2009). It was proposed that acid-catalysed glycolysis of crystallites occurs through a peeling reaction at the accessible cellulose reducing ends on the crystallite surface.

The aim of the current study is to clarify the influence of the cellulose DP, structural features of the micro-fibrils, and crystallinity on the cellulose glycolysis, with emphasis on degradation of amorphous cellulose domains, degradation of crystalline cellulose by 'quantum mode' mechanism, and the reaction kinetics. For this purpose, microcrystalline cellulose (DP = 470), Whatman filter paper no.1 (DP = 4320), and cotton linters (DP = 11790) were treated with ethylene glycol under catalysis of *p*-toluene sulfonic acid monohydrate at the different temperatures.

EXPERIMENTAL

Materials

Microcrystalline cellulose (MC, DP = 470, Acros Organics), purified cellulose sheets (Whatman filter paper, WH, DP = 4320), and cotton linters (CT, DP = 11790, Radeče, Slovenia) were used without any pretreatment. Ethylene glycol (EG, Merck), *p*-toluene sulfonic acid monohydrate (PTSA, Acros Organics), *N*,*N*-dimethylacetamide for HPLC (DMAc, Fluka), lithium chloride (LiCl, Acros Organics), dried before use at 180 °C in vacuum for 24 h and kept in desiccator), and sodium hydroxide (NaOH, Merck) were of reagent grade and were used without further purification.

Cellulose Degradation in Acidified Ethylene Glycol

Ten grams of cellulose, (dried at 105ºC for 24 h), 50g of EG, and 1.5g (3% w/w based on the EG) of PTSA as a catalyst were placed in a 250 cm^3 glass reactor (three necks), equipped with a mechanical stirrer. Cellulose liquefaction was carried out at

50°C, 90°C over 24 h, and at 150°C[1] over 4 h. Samples from the reaction mixture were taken at different time intervals and immediately cooled in an ice-bath. The acidity component was neutralized with 1 mol/L NaOH solution to prevent further cellulose degradation prior to product characterization.

Cellulose Residue Determination

Samples taken during the treatment were diluted with an excess of distilled water and vacuum-filtered through the filter paper, rinsed several time with DMAc and acetone, and dried in a vacuum at 50°C for 24 h. The residue content liquefaction was determined as the weight of the obtained dried solids relative to the starting amount of cellulose (Equation 1).

$$Residue\ content = (W_0 - W_t) / W_0 \quad (1)$$

Here, W_0 is the weight of starting cellulose, and W_t is the weight of residual cellulose.

FTIR Spectroscopic Analysis

The isolated residues were analyzed using a Perkin-Elmer Spectrum-1 (Perkin-Elmer, USA) FTIR spectrophotometer. The transmittance measurements were conducted using the KBr pellet method in a frequency range from 4000 cm^{-1} to 500 cm^{-1}.

X-ray Diffraction

X-ray diffraction (XRD) measurements were performed on a Siemens D5000 (Bruker, Germany) PANalytical X'Pert PRO (PANalytical, The Netherlands) system in order to estimate the crystalline-amorphous ratio of the initial cellulose samples and of the residues. The diffracted intensity of CuKα radiation (1.5406 Å) was measured in 2θ intervals between 10° and 30°.

Determination of the crystallinity index

The X-ray diffractograms of all samples were analyzed using the empirical procedure of Segal *et al.* (1959). The calculation of the crystallinity index (*Cr.I.*) followed Equation 2,

$$Cr.I.\ (\%) = (I_{200} - I_{am}) / I_{200} \times 100 \quad (2)$$

where, I_{200} is the maximum intensity of the diffraction from the (200) plane at $2\theta = 22.8°$ and I_{am} is the intensity of the amorphous background scatter measured at $2\theta = 18°$.

Determination of the crystallite width

The crystallite widths of both the original and the residual cellulose were estimated and evaluated using Scherrer equation (Equation 3) (Klug and Alexander 1974) from the peak profile of the (200) reflection at $2\theta = 22.8°$ that refers to the width of a crystallite (Andersson *et al.* 2003).

[1] Data were obtained for cellulose liquefaction at 150 °C with PTSA as a catalyst is reported in Jasiukaitytė *et al.* 2009 and used to compare cellulose degradations at all tested temperatures for reasons of clarity.

$$L = K\lambda/(\beta \cos\theta) \quad (3)$$

Here, L is the crystallite width, θ is the Bragg angle, λ is the wavelength of the radiation, K is a constant, and β is the corrected width of the peak given by the specimen. A value of $K = 0.9$ at half-width of the peak profiles was used.

The measured peak widths include the effects of crystallite size and instrumental broadening. The effect of instrumental broadening on the peak widths was assessed by measuring the peak width of a large undistorted crystal under identical operating geometries. The instrumental broadening amounted to 0.059° for the half-width where the silicon crystal was used as a sample (Warren and Biscoe 1938). The peak profiles were assumed to follow a Gaussian distribution.

Size-Exclusion Chromatography

Samples for size-exclusion chromatography were prepared as follows: the aliquot of a neutralized reaction mixture was mixed with distilled water, and any suspension of residual cellulose was filtered through a 0.45 μm polyamide membrane filter (Milipore). The obtained cellulose residue was rinsed several times with distilled water and dissolved in a LiCl/DMAc solvent system.

All the solutions of residual cellulose in LiCl/DMAc were filtered through the PTFE filters (0.45 μm) prior to injection. The LiCl concentration in the sample solutions was 1% (0.1 g of LiCl in 10 cm^3 of DMAc).

The HP - AGILENT system consisted of an isocratic pump HP 1100, refractive index detector AGILENT 1100 (detection cell temperature: 40°C), and column thermostat (temperature: 80 °C). The sample injection volume was 100 μL, and the sample concentration was 0.1%. The column used was PLgel 5 μm MIXED C 7.5 × 300 mm (Agilent). The eluent (1% LiCl/DMAc), filtered through the 0.45 μm polyamide membrane filter (Supelco), was pumped into the system at a flow rate of 0.5 cm^3/min. The calibration was performed with pullulan standards, which were prepared according the procedure used elsewhere (Strlič *et al.* 2002; Strlič and Kolar 2003). The chromatographic data were processed with PSS (Polymer Standards Service) WinGPC Unity software.

RESULTS AND DISCUSSION

In our previous study (Jasiukaitytė *et al.* 2009) on the cellulose degradation reaction in EG medium it was assumed that, due to the effects of H_2O being preferentially adsorbed by the cellulose, the reaction is analogous to hydrolysis. Accordingly, it was taken into account that approximately 5% (w/w based on cellulose) of H_2O is adsorbed by cellulose and an additional 9.4% (w/w based on PTSA) of H_2O is provided by the catalyst used for the degradation. It was determined that cellulose degradation in acidified EG begins with glycosidic oxygen protonation, followed by carbonium ion formation and scission of the glycosidic bond. Consequently, after the glycosidic bond cleavage, the

newly-appeared reducing cellulose chain ends were exposed to the glycosylation by ethylene glycol, followed by formation of 2-hydroxyethyl-D-glucopyranoside.

The combination of the high temperature, glycol concentration, and the amount of the catalysts caused particularly rapid degradation of the less-ordered cellulose segments and partial degradation of crystalline cellulose regions. The molecular weight distributions and the change of the crystallite size with time showed that the glycolysis of cellulose crystallites proceeded at the accessible cellulose reducing ends on the surface of the crystallites through a peeling reaction.

Weight Loss

Cellulose weight loss during the degradation in PTSA-acidified EG was evaluated by determination of not-solubilized cellulose residue. In order to assure that the obtained residue did not contain any cellulose derivatization products, samples were analyzed using FTIR spectroscopy. As expected, all of the analyzed samples exhibited the characteristic bands of cellulose: 3419-3342 cm^{-1} (OH stretching), 2901 cm^{-1} (CH stretching), 1430 cm^{-1} (CH_2 bending), 1371-1373 cm^{-1} (CH bending), and 1060-1031 cm^{-1} (CO stretching) (spectra not shown).

MC, WH, and CT residue contents during PTSA-catalyzed glycolysis at 50°C, 90°C, and 150°C are listed in Table 1. The intensive weight loss was observed for cellulose samples treated at 150°C, while the lower experimental temperatures apparently were insufficient to induce cellulose solvolysis.

Table 1. MC, WH, CT Residue Content during PTSA-Catalyzed Glycolysis at 50°C, 90°C, and 150°C, with Reaction Time

Time (min)	MC			WH			CT		
	50°C	**90°C**	**150°C**	**50°C**	**90°C**	**150°C**	**50°C**	**90°C**	**150°C**
5	0.996	0.996	0.869	0.980	0.989	0.859	0.982	0.971	0.858
15	0.997	0.998	0.749	0.975	0.970	0.749	0.995	0.965	0.849
45	0.991	0.985	0.483	0.982	0.968	0.596	0.978	0.959	0.724
120	0.987	0.983	0.169	0.993	0.979	0.385	0.986	0.983	0.511
240	0.992	0.989	0.130	0.971	0.981	0.149	0.990	0.981	0.281
1440	0.985	0.974		0.985	0.973		0.973	0.962	

By plotting weight loss ($L = (W_0-W_t)/W_0$) of MC, WH, and CT during the liquefaction at 150°C with time (Fig. 1), it was determined that the weight loss of celluloses (MC, WH, and CT) during the treatment follows first-order kinetics:

$$L = e^{-kt} \quad (4)$$

Here L is a weight loss, k is a rate constant, and t is time. A first-order kinetic model in terms of Equation 4 describes cellulose degradation in acid-catalyzed EG well enough, relative to the data available for the characterization of cellulose liquefaction in PTSA-catalyzed EG.

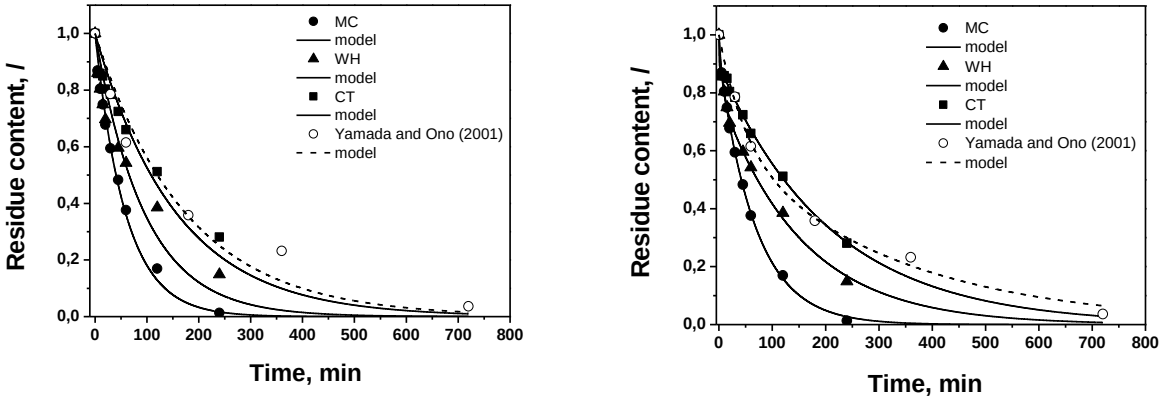

Fig. 1. MC, WH, CT residue content during PTSA-catalyzed glycolysis at 150°C with reaction time and re-elaboration of Yamada and Ono (2001) data of cellulose liquefaction H_2SO_4-catalyzed EG at 150°C. Fit using simple first-order kinetic model (Equation 4; *left*); Fit using sum first–order kinetic model under the constraint $L_a+L_c=1$ (Equation 5; *right*).

The rate constants of the cellulose weight loss were found to be reciprocal to the cellulose degree of polymerization. Here, the highest rate constants of the cellulose weight loss were determined for the cellulose with the lowest degree of polymerization. Jasiukaitytė *et al.* (2009) confirmed that cellulose degradation by acid-catalyzed glycolysis proceeds at the reducing cellulose chain ends. Accordingly, due to the lowest degree of polymerization of MC (DP = 470) and consequently the highest number of reducing chain ends available for the ethylene glycol attack, the lowest residual cellulose amount was obtained at the end of the treatment (after 240 min).

The comparison of the rate constants of the MC, WH, and CT weight loss was done with the data available in the literature. The rate constant of the cellulose weight loss during the liquefaction in H_2SO_4-catalyzed EG at 150°C was determined by re-elaboration of the results of Yamada and Ono (2001). The determined rate constant (5.80 x 10^{-3} min^{-1}) was similar to that of CT (6.42 x 10^{-3} min^{-1}) and thus may imply a similar cellulose weight loss mechanism during the liquefaction in H_2SO_4-catalyzed EG. The overall rate constant of the cellulose weight loss does not provide any information about the rate of the weight loss in amorphous and crystalline regions separately. In order to describe cellulose weight loss mechanism during the liquefaction at 150°C, the experimental data was additionally computed using a first-order kinetic law:

$$L = L_a(1-e^{-kat}) + L_c(1-e^{-kct}) \quad (5)$$

Here L is the fractional weight loss ($L = (W_0-W_t)/W_0$), and L_a and L_c are the asymptotic weight losses of amorphous and crystalline regions, respectively. L_a and L_c should be proportional to their initial relative amount. It is evident from the data plotted in Fig. 1 that MC degrades completely; therefore the curve fitting exercise for MC, WH, and CT was performed under the constraint $L_a + L_c = 1$.

The obtained values of L_a and L_c are listed in Table 2 and were very close to the initial XRD crystallinity data (Table 3) of the cellulose samples, especially for MC and

WH. In contrast to MC and WH L_a value similarity to the initial XRD crystallinity, L_a value determined for CT was 0.1, which was approximately 50% less than the content of the amorphous cellulose revealed by XRD. A crystallinity of the CT sample of about 91% was achieved in 5 min and remained relatively stable with treatment time. The L_a of 0.1 determined using Equation 5 could be interpreted in terms of the intensive initial amorphous cellulose solubilisation (liquefaction), which is confirmed by a significantly higher k_a value compared to the ones of MC and WH.

From the k_a and k_c values listed in Table 2 it is evident that the liquefaction of the amorphous cellulose regions proceeds 6(MC), 21(WH), and 57(CT) times faster compared to the liquefaction of the crystalline cellulose segments. Values of k_a increase with the increase of cellulose degree of polymerization, while k_c values, by contrast, decrease. Assuming that the amorphous cellulose chains extend through crystalline segments, the amorphous segments on the longer original chain due to the larger surface area are more susceptible to the liquefaction compared to those extended through the chains with lower degree of polymerization. The decrease of the k_c values could be influenced by size of the crystallites (Table 3). The smallest crystallites of MC due to the larger surface area exposed to the EG attack were accordingly solubilised with the highest k_c, while for larger crystallites of WH and CT, k_c values were respectively lower.

Table 2. Average Polymerization Degrees (DP) and Liquefaction Rate Constants (k) of MC, WH, CT, and Wood in PTSA-Catalyzed Ethylene Glycol at 150 °C.

Cellulose	k^a, min^{-1}	R^2	k_a, min^{-1}	k_c, min^{-1}	R^2	$L_a/(L_a+L_c)$
Microcrystalline cellulose (MC) DP 470	1.71×10^{-2}	0.9525	6.73×10^{-2} 7.68×10^{-2}	1.13×10^{-2} 1.30×10^{-2}	0.9532 0.9528	0.208[c] 0.167[d]
Whatman filter paper No.1 (WH) DP 4320	1.05×10^{-2}	0.9206	1.38×10^{-1} 1.30×10^{-1}	6.45×10^{-3} 6.27×10^{-3}	0.9169 0.9173	0.211[c] 0.218[d]
Cotton linters (CT) DP 11790	6.42×10^{-3}	0.8000	2.73×10^{-1} 4.45×10^{-2}	4.82×10^{-3} 3.95×10^{-3}	0.7957 0.7957	0.1[c] 0.202[d]
Commercial cellulose[b]	5.80×10^{-3}	0.9916	2.12×10^{-2} -	3.17×10^{-3} -	0.9916 -	0.364[c] -

[a] Rate constant (k) is calculated from Fig. 1, L = exp(-kt)

[b] Re-elaboration of Yamada and Ono (2001) data of cellulose liquefaction in H_2SO_4-catalyzed EG at 150°C

[c] Set as variable (Fig. 1; *right*)

[d] Initial XRD crystallinity

The values of L_a, L_c, k_a, and k_c for cellulose liquefaction in H_2SO_4-catalyzed EG at 150°C were determined from re-elaborated data of Yamada and Ono (2001) using Equation 5. The initial relative amount of amorphous cellulose (L_a) was significantly higher than the L_a determined for MC, WH, and CT. As expected, the larger quantity of the amorphous cellulose segments required a longer period of time to achieve the liquefaction, as confirmed by the smallest k_a value (3.17×10^{-3}) listed in Table 2.

However, the crystalline cellulose regions were liquefied with k_c of the same order of magnitude as WH and CT.

Two-parameter curve fitting using L_a and L_c determined by XRD was performed in order to compare k_a and k_c values. As expected, k_a and k_c for MC and WH were very close to those obtained from a three-parameter fitting curve where L_a was set as a variable, while the increase of the L_a in CT accordingly reduced k_a and increased the k_c values for CT. Consequently, the k_a and k_c values were obtained to be very close to the ones determined for commercial cellulose, which therefore implies the presence of the similar weight loss mechanism.

Cellulose Crystallinity and Crystallite Size

To understand the mechanism of MC, WH, and CT degradation in PTSA-catalyzed EG at different temperatures, the change of cellulose crystallinity and the average widths of crystallites were evaluated using the empirical procedure of Segal *et al.* (1959) and using the Scherrer equation (Klug and Alexander 1974), respectively. The minor changes of the crystallite widths (Table 3) followed by the significant weight loss, especially during the treatment at 150°C, implies the presence of the 'quantum mode' cellulose degradation mechanism. Rate constants of the crystalline region weight loss (k_c) determined through evaluation of the weight loss kinetics during the MC, WH, and CT liquefaction were found to increase with the enlargement of the crystallite surface area exposed to the EG attack. Additionally, the observed deviations between the widths of the crystallites with the treatment time indicate crystallite surface erosion rather than the degradation through the peeling pathway.

The highest crystallinity and crystallite width values were achieved in 5 min of the treatment at 150°C as a result of the rapid amorphous cellulose degradation. Furthermore, due to the induced crystallite surface erosion, crystallinity and crystallite width of MC and WH decreased gradually, while that of CT remained relatively the same with the reaction time. The considerable reduction of WH crystallite width (from 6.8 nm to 6.1 nm) as well as crystallinity decrease (from 92.6% to 71.3%) implies WH crystallites to be the most susceptible to the degradation in PTSA-catalyzed EG. From the obtained results it can be assumed that crystallinity is the determinant factor for WH (k_c = 6.45 x 10^{-3} min^{-1}) and CT (k_c = 4.82 x 10^{-3} min^{-1}) liquefaction.

In contrast to the WH crystallite degradation, there were not any appreciable changes observed for MC, neither in crystallite width (from 5.1 nm to 5.0 nm) nor in crystallinity (from 83.3% to 85.0%). Therefore, the highest value of k_c (1.13 x 10^{-2} min^{-1}) suggests that MC in PTSA-catalyzed EG (150°C) undergoes degradation through the 'quantum mode' mechanism.

During the MC, WH, and CT treatment at the lower experimental temperatures (50°C and 90°C) an increasing trend for the crystallites' width as well as crystallinities was observed. Due the absence of the cellulose weight loss the gradual growth of the crystallites' width and crystallinities could be interpreted in terms of scission-reordering in regenerated cellulosic fibres, as has been extensively studied by Ibbett *et al.* (2008). According to the cited authors, the scission-reordering occurs within disordered polymer regions at lateral crystal interfaces, which are accessible to aqueous agents through the pore spaces and polymer-free volume. This process is distinct from that of oligomer

solubilisation, which occurs within disordered polymer regions in series between crystal domains at the higher experimental temperatures (150°C), where no effective template exists for recrystallization.

Table 3. Crystallinity (%) and Width Changes of the Crystallites (nm) of Residual MC, WH, and CT Cellulose with Treatment Time

Crystallite Width (nm)									
Time (min)	50 °C			90 °C			150 °C		
	MC	WH	CT	MC	WH	CT	MC	WH	CT
0	5.1	6.8	6.4	5.1	6.8	6.4	5.1	6.8	6.4
5	5.0	7.4	6.5	5.4	8.1	7.5	5.3	7.1	6.7
60	6.0	7.7	7.5	5.5	7.9	6.8	5.1	6.9	6.7
120	5.6	8.0	6.8	5.4	7.9	6.8	5.2	6.9	6.6
240	5.5	7.7	7.8	5.6	7.7	7.7	5.0	6.1	6.6
1440	5.5	7.7	7.8	5.6	7.7	7.7	-	-	-
Time (min)	Crystallinity (%)								
0	83.3	78.2	79.8	83.3	78.2	79.8	83.3	78.2	79.8
5	85.8	86.9	84.7	83.2	87.4	81.0	87.5	92.6	91.9
60	86.6	84.6	87.3	83.0	90.4	89.0	86.6	92.3	92.0
120	86.7	86.6	83.7	81.5	91.9	91.8	86.5	90.9	92.0
240	86.4	85.0	87.1	85.5	92.6	86.4	85.0	71.3	90.5
1440	86.6	88.1	87.6	86.2	91.6	87.6	-	-	-

Molecular Mass Distributions

The products of the cellulose degradation in EG under catalysis of PTSA were monitored using size-exclusion chromatography (SEC). Average molecular mass (M) of the residual cellulose samples, taken at different time intervals, was determined by SEC, calibrated relative to pullulan standards.

Molecular mass distributions obtained by size-exclusion chromatography enable one to understand the mechanism of cellulose degradation by acid-catalyzed glycolysis. It was reported by Guaita *et al.* (1990) that polymer degradation proceeds purely randomly when the polydispersity (DP_w/DP_n) of the distribution of molecular mass approaches a value of 2 and remains constant during the degradation process. According to the authors, the polydispersity would fall below 2 if the scissions were primarily in the centre of the chains.

Polydispersities (DP_w/DP_n) evaluated from our experimental data are presented in Table 4. The ratios generally decrease with time as the average molecular mass decreases, initially from about 5.7 to about 2.6 for cellulose samples during the degradation in acidified EG. There is evidence of the ratios decreasing towards 2, which confirms that the degradation of MC, WH, and CT in ethylene glycol proceeds randomly without any preferential breakdown of the longest cellulose chains.

At the beginning of MC, WH, and CT degradation at 50°C, the increase of polydispersities was observed. The reason for the increased polydispersities is the

formation of the low-molecular mass fragments during degradation, while the intensive DP_w/DP_n increase in the case of CT (DP = 11790) degradation might be attributed to the nonhomogeneous degradation kinetics of limited cellulose domains.

Table 4. Average Polymerization Degrees (DP_w, DP_n) and Polydispersities (DP_w/DP_n) of the Initial and Residual Cellulose Samples with Time of Degradation in EG with PTSA as a Catalyst at 50°C, 90°C, and 150°C

Time (min)	MC			WH			CT		
	DP_w	DP_n	DP_w/DP_n	DP_w	DP_n	DP_w/DP_n	DP_w	DP_n	DP_w/DP_n
50 °C									
0	470	82	5.73	4320	937	4.61	11790	2136	5.52
5	468	60	7.95	3420	453	7.58	9790	550	17.96
15	432	66	6.58	2772	473	5.86	5861	324	18.85
30	421	83	5.06	2341	416	5.75	4214	258	18.23
60	405	75	5.40	1890	369	5.16	2582	264	9.82
120	402	80	5.02	1354	321	4.22	2188	215	10.25
240	399	79	5.05	1081	253	4.28	1295	174	7.52
480	390	74	5.31	724	199	3.64	820	126	6.56
1440	344	69	4.98	504	138	3.69	500	72	6.95
90 °C									
5	386	67	5.81	814	185	4.40	937	180	5.28
15	353	65	5.45	591	129	4.59	742	160	4.65
30	338	61	5.60	385	101	3.82	420	104	4.10
60	318	62	5.12	313	91	3.44	351	87	4.01
120	296	56	5.27	284	75	3.79	289	70	4.36
240	305	62	4.94	271	67	4.04	294	69	4.24
480	283	59	4.77	266	70	3.82	283	81	3.51
1440	257	54	4.80	262	71	3.68	280	81	3.48
150 °C									
1	330	84	3.91	336	97	3.46	342	99	3.47
5	254	63	4.05	278	84	3.32	299	89	3.36
15	211	54	3.92	278	87	3.19	283	87	3.25
60	167	50	3.37	271	91	2.97	270	99	2.73
120	146	46	3.17	276	97	2.85	262	101	2.59
240	143	48	2.97	272	92	2.96	264	103	2.57

SEC of Cellulose Solutions after Degradation in PTSA-Catalyzed EG at Different Reaction Temperatures

WH (DP = 4320) and CT (DP = 11790) degradation

SEC chromatograms of the residual cellulose samples demonstrated an analogous degradation pathway for WH (DP = 4320) and for CT (DP = 11790), while MC (DP =

470), due to the different surface morphology, behaved differently. As an example, chromatograms (normalized to the sample weight) of WH (DP = 4320) and of residual cellulose from this sample, taken at the different time intervals of degradation at 50 °C are shown in the Fig. 2. Throughout the WH degradation in acidified EG at 50 °C (Fig. 2), the main peak with the broad weight distribution was gradually shifting to a lower molecular mass with time, consequently obtaining more narrow molecular mass distributions.

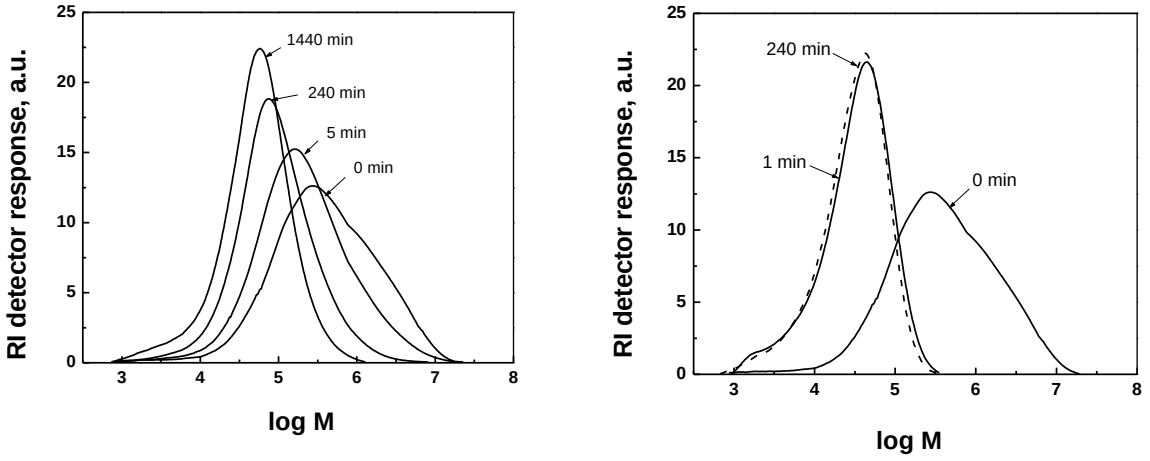

Fig. 2. SEC chromatograms of WH (DP = 4320) and of the samples, taken at the different time intervals: 50 °C (left); 150 °C (right)

During the first 5 minutes of cellulose degradation at 50 °C, the initial average polymerization degree of WH decreased from 4320 to 3420, and for CT the observed decrease was from 11790 to 9790 (Table 2). The initial drop in the cellulose molecular mass represents the primary scissions of 'weak links' (Nevell 1985), covalent bonds together with the breakdown of inter-chain hydrogen bonds and intra-chain hydrogen bonds. The degradation of the WH and CT cellulose further proceeds in a random fashion by undergoing cleavage of the glycosidic linkages in the less ordered (amorphous) cellulose regions. The hydrolytic chain-breaking in amorphous fragments that are extended through crystalline segments proceeds gradually without producing larger oligomers, which would otherwise appear as the low-molecular mass material (shoulder) in SEC chromatograms.

Analogous degradation trend of WH-90 and CT-90 in EG-PTSA was observed from SEC chromatogram profiles. The appearance of the additional low-molecular mass shoulder in the chromatogram of the sample, taken after 240 min of the degradation indicates the presence of the larger cellulose oligomers, as was suggested by Stephens *et al.* (2008). The newly formed fragments were composed of approximately 12 glucose units and were similar to the ones formed during the WH-150 and CT-150 degradation in EG-H_2SO_4 and EG-PTSA systems, which were described by Jasiukaitytė *et al.* (2009) in terms of amorphous fraction reorientation and crystallization. The formation of free cellulose oligomers started after approximately 120 min of treatment, when DP_w was

approaching the value of 284 and 289; thus the appearance of the low-molecular mass material increased the DP_w/DP_n ratios of the samples to 3.79 and 4.36, respectively (Table 2). The weight-average polymerization degree did not decrease as rapidly as it was observed during the previous 120 min of the reaction. Despite the same WH and CT degradation pathway, the influence of cellulose DP may be clearly seen after 240 min from the SEC chromatogram profiles depicted in Fig. 3. Under the identical reaction conditions for WH and CT, the hydronium ion concentration is capable of initiating a similar amount of scission per cellulose chain. Consequently, the lower initial DP and crystallinity values of WH enabled the formation of a larger amount of smaller cellulose segments, which is confirmed by the increased main peak intensity and narrower molecular mass distribution after 240 min of treatment in comparison to the CT.

The influence of cellulose polymerization degree on the WH and CT degradation is clearly observable through the low-molecular mass shoulder formation trend. This shoulder observed in the SEC chromatogram profile after 240 min of WH-90 degradation indicates the appearance of free cellulose oligomers, which are obtained after the degradation of the dangling amorphous tie-chain fragments. Due to the absence of the cellulose weight loss, the amount of the low-molecular mass material grows with the prolonged WH-90 degradation, consequently increasing the intensity of the shoulder in the SEC chromatogram profile of the sample taken after 24 h of the treatment. In contrast to the WH-90 degradation, the low-molecular mass shoulder observed after 240 min of CT-90 degradation is slightly shifted towards the high molecular masses, thus indicating the formation of the larger free cellulose oligomers. Furthermore, the change of the shoulder shape and the shift towards the low-molecular masses after 24 h of CT-90 treatment confirmed the occurrence of further chain-breaking of already broken amorphous tie-chains near the ends of the amorphous chain segments.

The degradation of WH and CT at 150°C followed a similar pathway (Jasiukaitytė *et al.* 2009). The considerable shift of the WH peak with broad weight distribution after 1 min of treatment at 150 °C to the low-molecular mass is evident in Fig. 2. The increased intensity of the main peak with narrow weight distribution and appearance of low-molecular mass shoulder was exactly the same as it was obtained after 240 min of WH degradation at 90ºC. Therefore, it can be concluded that at the lower experimental temperature, WH and CT degradation proceeds in a similar manner. However, in contrast to the WH-90 and CT-90 degradation, the formation of soluble low-molecular mass compounds followed by WH and CT weight loss at 150°C, resulted in a loss of the low-molecular mass shoulder during the prolonged time of the treatment (Fig. 2).

MC (DP = 470) degradation

During the first 5 min of the MC degradation, the initial DP of 470 decreased to 468 at 50°C and to 386 at 90°C (Table 2). The degradation of the MC at the lower experimental temperatures (MC-50 and MC-90) proceeds in a similar manner, while during liquefaction at 150°C, MC degradation proceeds differently. This can be deduced from the SEC chromatograms of the initial MC and of the samples, taken at different treatment times, as shown in Fig. 4.

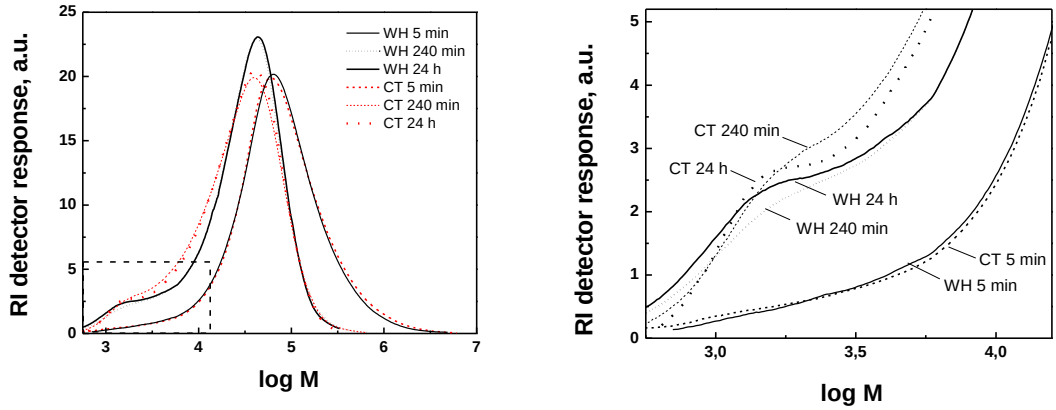

Fig. 3. SEC chromatograms of WH and CT samples, taken after 5 min, 240 min, and 24 h of degradation in PTSA-catalyzed EG at 90 °C (left); Enlargement of the low-molecular mass shoulder in SEC chromatograms of WH and CT samples, taken after 240 min and 24 h of degradation (right)

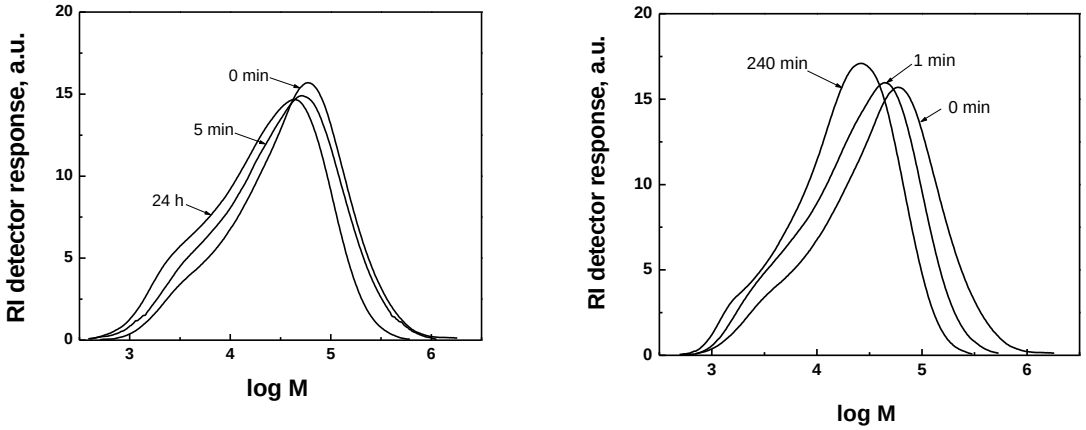

Fig. 4. SEC chromatograms of MC (DP = 470) and of the samples, taken at the different time intervals: MC at 90°C (right); MC at 150°C (left)

At the lower experimental temperatures, MC undergoes ordinary degradation. The decrease of the main peak intensity and shift to lower-molecular mass with time could be interpreted in terms of amorphous fraction degradation or more likely shortening of chains due to the degradation of dangling amorphous or paracrystalline ends that compete with random degradation. The absence of weight loss and increase of the low-molecular mass shoulder during MC degradation at 90°C, in particular, implies the presence of the shorter MC chains (Fig. 4). The lower experimental temperatures are insufficient to induce solvolysis of low-molecular mass MC fragments that accordingly enlarges molecular mass distribution. The increase of the polydispersities at the beginning of the MC treatment at 50°C (Table 2) shows slower degradation of amorphous ends compared to MC degradation at 90°C.

During the first minute of MC degradation at 150°C, the initial DP of 470 decreased to 330. In contrast to the MC-90 degradation, the slight increase of the main peak intensity and the appearance of the low-molecular mass shoulder already after 1 min of the MC treatment at 150°C indicate a similar MC degradation pathway as at 90°C. Furthermore, some chains in the crystalline regions degrade completely and became soluble, causing great weight loss. As a result, the increase of the main peak intensity with evidently reduced low-molecular mass shoulder was observed in the chromatogram of MC sample after 240 min (Fig. 4). In addition, due to the induced solvolysis of the low-molecular mass fragments, samples with significantly reduced polydispersities were obtained (Table 2).

The loss of 98.7% of MC weight during the 240 min treatment at 150°C, while DP decreased only from 470 to 145, shows that MC degradation proceeds via 'quantum mode' mechanism (Calvini 2005). From the obtained results, it is clear that MC retains its relatively long chains and accordingly MC crystallites tend to decrease in quantity resulting in soluble low-molecular mass fragments.

Kinetics of the Cellulose Degradation in Acidified Ethylene Glycol

Traditionally, to evaluate kinetics of cellulose degradation, the Ekenstam equation (Ekenstam 1936; pseudo-zero order) is applied:

$$1/DP_t - 1/DP_0 = kt \quad (4)$$

Here k is the reaction rate constant, and DP_t and DP_0 are the polymerization degrees at times t and 0, respectively. In the current study of cellulose degradation in acidified EG, this approach was not applied due to evidently strong deviations from linearity in plots. In addition, the limited applicability of the Ekenstam equation due to a deviation from linearity – upward or downward curvature – has been reported by several authors as well (Bicchieri and Pepa 1996; Bogaard and Whitmore 2001).

A general first-order kinetic model was used to describe Whatman filter paper (WH; $DP_0 = 4320$) and cotton linters (CT; $DP_0 = 11790$), degradation at 50°C, 90°C and 150°C in order to determine cellulose DP influence on the cellulose degradation kinetics (Equation 5).

$$\ln(1-1/DP_o) - \ln(1-1/DP_t) = kt \quad (5)$$

In order to minimize errors due to the polydispersity ratios, the cellulose degradation by acid-catalyzed glycolysis was evaluated by plotting the number of scissions per anhydroglucose unit ($1/DP - 1/DP_0$) against time, as was suggested by Calvini *et al.* (2008) in terms of Equation 6.

$$S = 1/DP - 1/DP_0 \text{ (scissions per anhydroglucose unit)} \quad (6)$$

Here, DP_t and DP_o are the polymerization degrees at times t and 0, respectively. Authors developed a first-order kinetic relation (Equation 7), where n^o is the initial amount of cellulose bonds per anhydroglucose unit ($n^o = 1-1/DP_o$), k is the rate constant.

$$S = n^o (1 - e^{-kt}) \quad (7)$$

However, Equations 4 and 5 hold for the degradation in homogeneous medium, where all the cellulose bonds are available for the degradation (Krassig 1985). In heterogeneous medium of WH and CT degradation in PTSA-catalyzed EG, the influence of the levelling-off degree of polymerization (LODP) was taken into account, since amorphous bonds degraded rather easily until LODP values of 267 (WH) and 272 (CT), as was shown by the rapid decrease of DP with limited weight loss. Further WH and CT degradation would require drastic conditions and accordingly would follow a different degradation pathway. Thus, in heterogeneous medium Equation 7 should be written as

$$(1/DP - 1/DP_0) = (1/LODP - 1/DP_0) \times (1-e^{-kt}) \quad (8)$$

MC degradation in acidified ethylene glycol proceeds through the quantum mode mechanism. Here, crystallites degrade in quantity, resulting in soluble low-molecular mass fragments and still retain relatively long chains even at 150°C. At the lower experimental temperatures, the shortening of chains due to the degradation of dangling amorphous ends compete with the random degradation. Due to the low initial DP and amount of scissions per chain, this competitive reaction immediately influence the DP values of MC, while it is practically negligible for the WH and CT samples and its effect is observable only at the end of the reaction. Therefore, DP values determined during MC degradation were not suitable for the evaluation of the reliable cellulose degradation kinetics. It should be noted that all scissile units (n_0) were calculated according to the reached LODP at the end of the individual degradation. In case of WH and CT degradation at 50°C, LODP value was evaluated from data obtained at 90°C and 150°C. The values of k have been estimated with the aid of non-linear curve fitting software (Origin 60 of the OriginLab Co.) assuming that all bonds in cellulose degraded at the same rate (Fig. 5; Table 5).

As expected, due to the parameters such as multiple zone kinetics in limited domains, influence of impurities, and/or already oxidised spots deviations were observed. Obviously, 50°C was an insufficient temperature to assure a semi-homogeneous degradation in heterogeneous samples and to reach LODP in 1440 min. Re-elaboration of Lauriol *et al.* (1987) data through the same equation showed very good fit, using single first-order kinetics. Additionally, from the data presented in Fig. 6 it is evident that WH and CT during the PTSA-catalyzed treatment at 50°C follow the identical degradation pathway as cellulose investigated by Lauriol *et al*. (1987). Therefore, it could be assumed that in order to achieve LODP of WH and CT at 50°C, the prolonged treatment time is needed.

A temperature increase of 100°C increased the rate of WH and CT degradation by approximately 615 and 750 times, as shown by the rate constants listed in Table 5. The degradations of WH and CT in acidified EG followed the Arrhenius relationship over the temperature range of 50 to 150 °C. The activation energies (E_a) for WH and CT degradations determined from the slope of the plots *lnk* vs. *1/T* were 65.7 and 63.9 kJ/mol, respectively. Analogous activation energies of WH and CT degradation imply the

transfer of the equivalent required energy to each molecule to cause the reaction to proceed, independent of cellulose degree of polymerization.

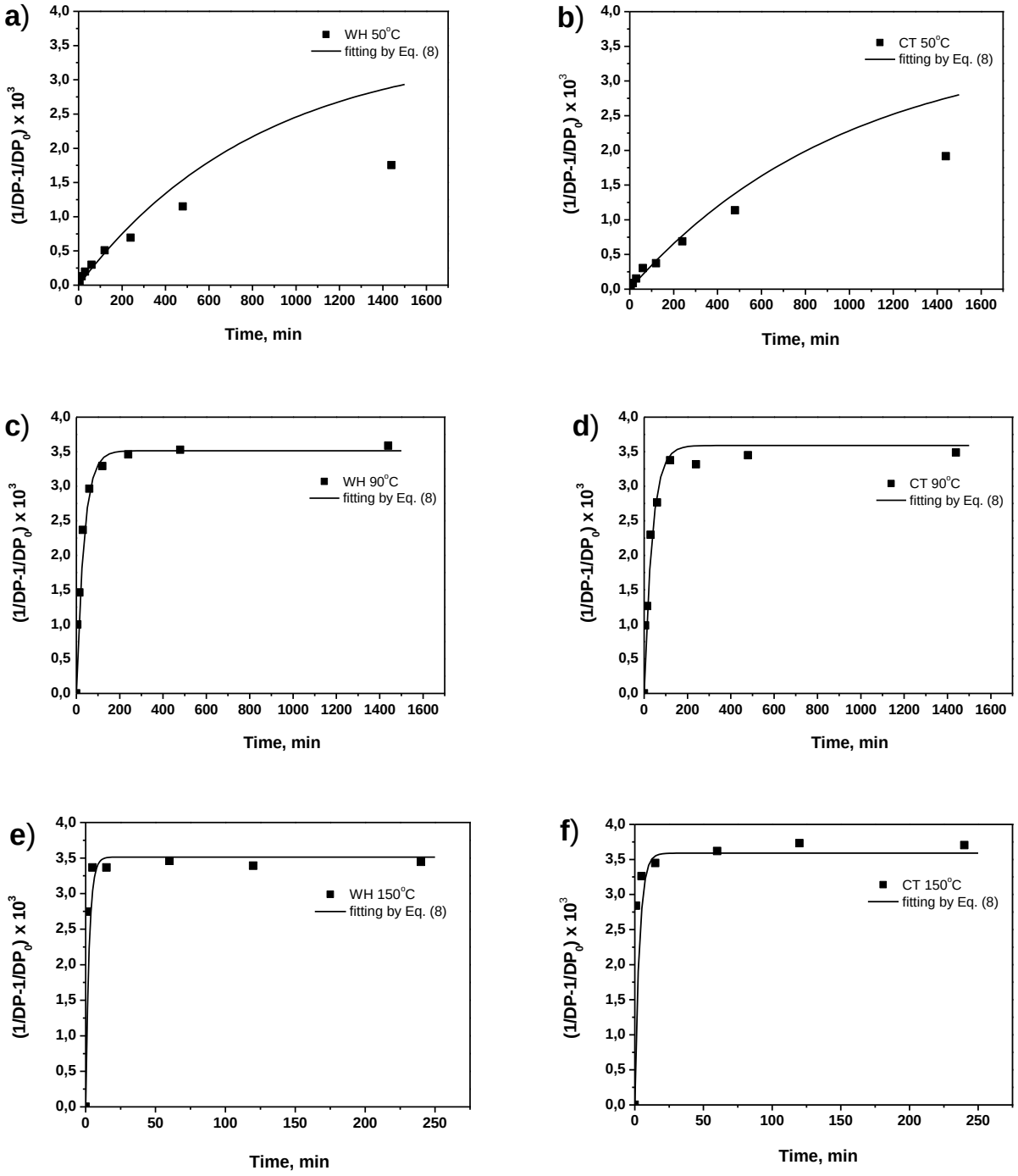

Fig. 5. Experimental data of WH (**a; c; e**) and CT (**b; d; f**) degradation at 50°C, 90°C, and 150°C in acidified EG fit using simple first-order kinetic model (Equation 8). Scissions per anhydroglucose unit ($S = 1/DP - 1/DP_0$) versus reaction time

Table 5. Summary of MC (DP_0 = 470), WH (DP_0 = 4320), and CT (DP_0 = 11790) Glycolysis as Determined by Equation 8

		50 °C	90 °C	150 °C*	E_a (kJ/mol)
WH	DP_0	4320	4320	4320	
	k (min^{-1})	2.6×10^{-3}	3.7×10^{-2}	1.6	65.7 ± 2.5
	R^2	0.8125	0.8702	0.8291	
	LODP	267**	262 (267**)	272 (267**)	
CT					
	DP_0	11790	11790	11790	
	k (min^{-1})	2.0×10^{-3}	3.3×10^{-2}	1.5	63.9 ± 2.5
	R^2	0.7663	0.8595	0.9480	
	LODP	272**	280 (272**)	264 (272**)	
Lauriol					
	DP_0	4700			
	k (min^{-1})	6.0×10^{-4}			
	R^2	0.7935			
	LODP	250			

*The degradation of cellulose at 150 °C lasted for 240 min
**Value is an average of the LODP values at 90°C and at 150°C and used for n_0 calculation.

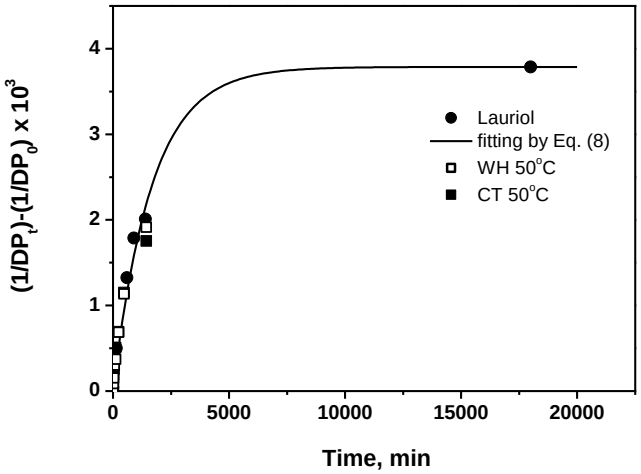

Fig. 6. Experimental data of WH and CT degradation at 50°C in acidified EG and re-elaborated Lauriol *et al.* (1987) data of cellulose hydrolysis in 1N HCl at 50°C fit using simple first-order kinetic model (Equation 8). Scissions per anhydroglucose unit (S = 1/DP - 1/DP_0) versus reaction time.

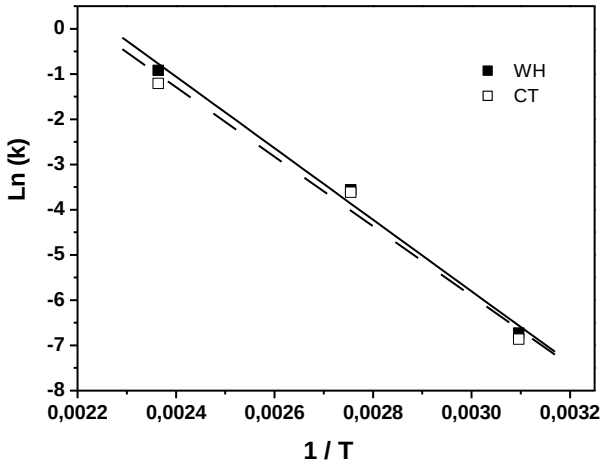

Fig. 7. Arrhenius plot for the DP reduction rates of WH (R^2 = 0,9958) and CT (R^2 = 0,9923) glycolysis (3 wt% EG) vs. inverse temperature (K°) in the range 50 to 150°C.

CONCLUSIONS

1. The cellulose weight loss mechanism during liquefaction at 150°C was computed using a first-order kinetic law. The determined asymptotic weight losses of amorphous and crystalline regions in microcrystalline cellulose (MC) and Whatman filter paper no.1 (WH) were proportional to their initial relative amount determined by X-ray diffraction. Liquefaction of the amorphous cellulose regions was 6 (for MC), 21 (for WH), and 57 for cotton linters (CT) times faster compared to the liquefaction of the crystalline cellulose segments. The rate of amorphous cellulose weight loss increased with cellulose degree of polymerization, while the rate of crystalline cellulose weight loss was reciprocal to the size of the crystallites.
2. Degradation of MC proceeded via a 'quantum mode' mechanism. Despite the loss of 98.7% of the weight during the treatment, MC retained its relatively long chains. MC crystallites tend to decrease in quantity through surface erosion, resulting in soluble low-molecular weight products.
3. Degradation of WH and CT in ethylene glycol proceeded randomly without any preferential breakdown of the longest cellulose chains, independent of the starting polymerization degree, crystallinity, and treatment temperature. Nevertheless, at the lower experimental temperature of 90°C, a larger amount of smaller segments were formed from the cellulose with lower initial polymerization degree and crystallinity (WH), which accordingly were more susceptible for the liquefaction at 150°C, as was confirmed by a higher rate constant of the weight loss constant compared to CT.
4. Cellulose degradation at the lower temperatures could be used for cellulose (lingo-cellulosics) pre-treatment that would facilitate liquefying agent penetration into the crystalline cellulose regions and consequently reduce time required for the lignocellulosic biomass liquefaction.
5. A good experimental data fit was achieved using a first-order kinetic model, which characterizes cellulose degradation in heterogeneous media. However, the lower determination coefficient values imply the limited applicability of the selected model to describe WH and CT degradation at different temperatures.
6. Analogous activation energies of WH and CT degradation in acidified ethylene glycol imply the degradation to progress independently from the cellulose degree of polymerization.

ACKNOWLEDGMENTS

The authors acknowledge the financial support from the Ministry of Higher Education, Science and Technology of the Republic of Slovenia and Slovenian Research Agency (programme P2-0145).

REFERENCES CITED

Alma, M. H., Maldas, D., and Shiraishi, N. (1998). "Liquefaction of several biomass wastes into phenol in the presence of various alkalis and metallic salts as catalysts," *J. Polym. Eng.* 18, 162-177.

Andersson, S., Serimma, R., Paakkari, T., Saranpää, P., and Pesonen, E. (2003). "Crystallinity of wood and the size of cellulose crystallites in Norway spruce (*Picea abies*)," *J. Wood Sci.* 49, 531-537.

Bicchieri, M., and Pepa, S. (1996). "The degradation of cellulose with ferric and cupric ions in a low-acid medium," *Restaurator* 17, 165-183.

Bogaard, J., and Whitmore, P. M. (2001). "Effects of dilute calcium washings treatments on paper," *J. Am. Inst. Conser.* 40, 105-123.

Calvini, P. (2005). "The influence of levelling-off degree of polymerisation on the kinetics of cellulose degradation," *Cellulose* 12, 445-447.

Calvini, P., Gorrassini, A., and Merlani, A. L. (2008). "On the kinetics of the cellulose degradation: looking beyond the pseudo zero order rate equation," *Cellulose* 15, 193-203.

Ekenstam, A. (1936). "The behavior of cellulose in mineral acid solution: Kinetic study of the decomposition of cellulose in acid solutions," *Chemische Berichte* 69, 553-559.

Guaita, M., Chiantore, O., and Luda, M. P. (1990). "Monte Carlo simulations of polymer degradations. 1. Degradations without volatilization," *Macromolecules* 23, 2087-2092.

Ibbett, R. N., Domvoglou, D., and Phillips, D. A. S. (2008). "The hydrolysis and recrystallisation of lyocell and comparative cellulosic fibres in solutions of mineral acid," *Cellulose* 15, 241-254.

Jasiukaitytė, E. (2010). "Identification of products obtained by acid catalyzed cellulose and lignin liquefaction with polyfunctional alcohols," *Ph.D. dissertation* University of Ljubljana.

Jasiukaitytė, E., Kunaver, M., and Strlič, M. (2009). "Cellulose liquefaction in acidified ethylene glycol," *Cellulose* 16, 393-405.

Klug, H. P., and Alexander, L. E. (1974). *X-Ray Diffraction Procedures: For Polycrystalline and Amorphous Materials*, H. P. Klug, and L. E. Alexander (eds.), John Wiley & Sons, New York.

Kobayashi, M., Asano, T., Kajiyama, M., and Tomita, B. J. (2004). "Analysis on residue formation during wood liquefaction with polyhydric alcohol," *J. Wood Sci.* 50, 407-414.

Krassig, H. (1985). *Cellulose and its Derivatives: Chemistry, Biochemistry and Applications*, J. F. Kennedy, G. O. Phillips, D. J. Wedlock, P. A. Williams (eds.), Ellis Horwood Limited Publishers, Chichester, U.K.

Kunaver, M., Jasiukaitytė, E., Čuk, N., and Guthrie, J. T. (2010). "Liquefaction of wood, synthesis and characterization of liquefied wood polyester derivatives," *J. Appl. Polym. Sci.* 115, 1265-1271.

Lauriol, J. M., Comtat, J., Froment, P., Pla, F., and Robert, A. (1987). "Molecular weight distribution of cellulose by on-line size exclusion chromatography – low angle laser light scattering Part. II. Acid and enzymatic hydrolysis," *Holzforschung* 41, 165-169.

Lin, L., Yoshioka, M., Yao Y., and Shiraishi, N. (1994). "Liquefaction of wood in the presence of phenol using phosphoric acid as a catalyst," *J. Appl. Polym. Sci.* 52, 1629-1636.

Lin, L., Yoshioka, M., Yao, Y., and Shiraishi, N. (1995). "Preparation and properties of phenolated wood/phenol/formaldehyde condenced resin," *J. Appl. Polym. Sci.* 58, 1297-1304.

Nevell, T. P. (1985). *Cellulose Chemistry and its Applications*, T. P. Nevel and S. H. Zeronian (eds.), John Wiley & Sons Inc., New York, N.Y.

Pan, H., Shupe, T. F., and Hse, C. Y. (2007). "Characterization of liquefied wood residues from different liquefaction conditions," *J. Appl. Polym. Sci.* 105, 3739-3746.

Segal, L., Creely, J. J., Martin, A. E., Conrad, J., and Conrad, C. M. (1959). "An empirical method for estimating the degree of crystallinity of native cellulose using the X-Ray diffractometer," *Text. Res.* 29, 786-794.

Stephens, C. H., Whitmore, P. M., Morris, H. R., and Bier, M. E. (2008). "Hydrolysis of the amorphous cellulose in cotton-based paper," *Biomacromolecules* 9, 1093-1099.

Strlič, M., and Kolar, J. (2003). "Size exclusion chromatography of cellulose in LiCl/*N*,*N*-dimethylacetamide," *J. Biochem. Biophys. Method.* 56, 265-279.

Strlič, M., Kolenc, J., Kolar, J., and Pihlar, B. (2002). "Enthalpic interactions in size-exclusion chromatography of pullulan and cellulose in LiCl-*N*,*N*-dimethylacetamide," *J. Chromatogr. A* 964, 47-54.

Warren, B. E., and Biscoe, J. (1938). "The structure of silica glass by x-ray diffraction studies," *J. Am.Ceram. Soc.* 21, 49-54.

Yamada, T., and Ono, H. (1999). "Rapid liquefaction of lignocellulosic waste by using ethylene carbonate," *Bioresour. Technol.* 70, 61-67.

Yamada, T., and Ono, H. (2001). "Characterization of the products resulting from ethylene glycol liquefaction of cellulose," *J. Wood Sci.* 47, 458-464.

Zhang, T., Zhou, Y., Liu, D., and Petrus, L. (2007). "Qualitative analysis of products formed during the acid catalyzed liquefaction of bagasse in ethylene glycol," *Bioresour. Technol.* 98, 1454-1459.

Article submitted: December 9, 2011; Peer review completed: January 23, 2012; Revised version received: May 17, 2012; Accepted: May 18, 2012; Published: May 24, 2012.